

**Original citation:**

Liga, Gabriele, Xu, Tianhua, Alvarado, Alex, Killey, Robert I. and Bayvel, Polina. (2014) On the performance of multichannel digital backpropagation in high-capacity long-haul optical transmission. *Optics Express*, 22 (24). 30053.

**Permanent WRAP URL:**

<http://wrap.warwick.ac.uk/93855>

**Copyright and reuse:**

The Warwick Research Archive Portal (WRAP) makes this work of researchers of the University of Warwick available open access under the following conditions.

This article is made available under the Creative Commons Attribution 4.0 International license (CC BY 4.0) and may be reused according to the conditions of the license. For more details see: <http://creativecommons.org/licenses/by/4.0/>

**A note on versions:**

The version presented in WRAP is the published version, or, version of record, and may be cited as it appears here.

For more information, please contact the WRAP Team at: [wrap@warwick.ac.uk](mailto:wrap@warwick.ac.uk)

# On the performance of multichannel digital backpropagation in high-capacity long-haul optical transmission

Gabriele Liga,\* Tianhua Xu, Alex Alvarado,  
Robert I. Killey and Polina Bayvel

*Optical Networks Group, Department of Electronic and Electrical Engineering,  
University College London, London WC1E7JE, UK*

[\\*g.liga@ee.ucl.ac.uk](mailto:g.liga@ee.ucl.ac.uk)

**Abstract:** The performance of digital backpropagation (DBP) equalization when applied over multiple channels to compensate for the nonlinear impairments in optical fiber transmission systems is investigated. The impact of a suboptimal multichannel DBP operation is evaluated, where implementation complexity is reduced by varying parameters such as the number of nonlinear steps per span and sampling rate. Results have been obtained for a reference system consisting of a  $5 \times 32$  Gbaud PDM-16QAM superchannel with 33 GHz subchannel spacing and Nyquist pulse shaping under long-haul transmission. The reduction in the effectiveness of the algorithm is evaluated and compared with the ideal gain expected from the cancellation of the nonlinear signal distortion. The detrimental effects of polarization mode dispersion (PMD) with varying DBP bandwidth are also studied. Key parameters which ensure the effectiveness of multichannel DBP are identified.

© 2014 Optical Society of America

**OCIS codes:** (060.1660) Coherent communications; (060.2330) Fiber optics communications.

---

## References and links

1. I. B. Djordjevic, M. Arabaci and L. L. Minkov, "Next generation FEC for high-capacity communication in optical transport networks," *J. Lightwave Technol.* **27**(16), 3518–3530 (2009).
2. I. B. Djordjevic, "Suppression of fiber nonlinearities and PMD in coded-modulation schemes with coherent detection by using turbo equalization," *J. Opt. Commun. Netw.* **1**(6), 555–564 (2009).
3. I. B. Djordjevic, "Advanced coded modulation for ultra-high speed optical transmission," in *Tech. Digest of Optical Fiber Communications*, 2014, paper W3J.4.
4. E. Ip, "Nonlinear compensation using backpropagation for polarization-multiplexed transmission," *J. Lightwave Technol.* **28**(6), 939–951 (2010).
5. E. M. Ip and J. M. Kahn, "Compensation of dispersion and nonlinear impairments using digital backpropagation," *J. Lightwave Technol.* **26**(20), 3416–3425 (2008).
6. E. M. Ip and J. M. Kahn, "Fiber impairment compensation using coherent detection and digital signal processing," *J. Lightwave Technol.* **28**(4), 502–519 (2010).
7. D. S. Millar, S. Makovejis, C. Behrens, S. Hellerbrand, R. I. Killey, P. Bayvel and S. J. Savory, "Mitigation of fiber nonlinearity using a digital coherent receiver," *J. Select. Topics Quant. Electr.* **16**(5), 1217–1226 (2010).
8. S. Benedetto and E. Biglieri, *Principles of Digital Transmission with Wireless Applications*, Chapter 8, (Kluwer Academic, 1999).
9. D. Rafique and A. Ellis, "Digital back-propagation for spectrally efficient WDM 112 Gbit/s PM m-ary QAM transmission," *Opt. Express* **19**(6), 5219–5224 (2011).
10. D. Rafique and A. Ellis, "Impact of signal-ASE four-wave mixing on the effectiveness of digital back-propagation in 112 Gb/s PM-QPSK systems," *Opt. Express* **19**(4), 3449–3454 (2011).

11. G. Gao, X. Chen and W. Shieh, "Influence of PMD on fiber nonlinearity compensation using digital back propagation," *Opt. Express* **20**(13), 14406–14418 (2012).
12. F. Yaman and G. Li, "Nonlinear impairment compensation for polarization-division multiplexed WDM transmission using digital backward propagation," *IEEE Photonics Journal* **2**(5), 816–832 (2010).
13. T. Tanimura, M. Nolle, J. K. Fischer and C. Schubert, "Analytical results on back propagation nonlinear compensator with coherent detection," *Opt. Express* **20**(27), 28779–28785 (2012).
14. I. P. Kaminow, T. Li and A. E. Willner, *Optical Fiber Telecommunications: Systems and Networks*, Vol. VIB, Chapter 5, (Academic Press, 2013).
15. R. Asif, C.-Y. Lin, M. Holtmannspoeetter and B. Schmauss, "Optimized digital backward propagation for phase modulated signals in mixed-optical fiber transmission link," *Opt. Express* **18**(22), 22796–22807 (2011).
16. C.-Y. Lin, A. Napoli, M. Kuschnerov, B. Spinnler, M. Bohn, D. Rafique, V. A. J. Sleiffer, and B. Schmauss, "Adaptive digital back-propagation for optical communication systems," in *Tech. Digest of Optical Fiber Communications*, 2014, paper M3C.4.
17. R. Rath, J. Leibrich, W. Rosenkranz, "On the optimization of link design using nonlinear equalization for 100 Gb/s 16QAM transmission," in *Tech. Digest of European Conference on Optical Communications*, 2012, paper P3.10.
18. E. F. Mateo, L. Zhou and G. Li, "Impact of XPM and FWM on the digital implementation of impairment compensation for WDM transmission using backward propagation," *Opt. Express* **16**(20), 16124–16137 (2008).
19. E. F. Mateo, X. Zhou and G. Li, "Improved digital backward propagation for the compensation of inter-channel nonlinear effects in polarization-multiplexed WDM systems," *Opt. Express* **19**(2), 570–583 (2011).
20. E. F. Mateo, F. Yaman and G. Li, "Efficient compensation of inter-channel nonlinear effects via digital backward propagation in WDM optical transmission," *Opt. Express* **18**(14), 15144–15154 (2010).
21. E. Ip, Y. K. Huang, Y. Shao, B. Zhu, D. Peckham, R. Lingle, "3 x 112-Gb/s DP-16QAM Transmission over 3580 km of ULAF with interchannel nonlinearity compensation," in *IEEE Photonic Society 24th Annual Meeting, WEE3* (2011).
22. E. Ip, Y. K. Huang, E. Mateo, Y. Aono, Y. Yano, T. Tajima and T. Wang, "Interchannel nonlinearity compensation for 3λ x 114 Gb/s DP-8QAM using three synchronized sampling scopes," in *Tech. Digest of Optical Fiber Communications*, 2012, paper OM3A.6.
23. N. K. Fontaine, X. Liu, S. Chandrasekhar, R. Ryf, S. Randel, P. Winzer, R. Delbue, P. Pupalakis and A. Sureka, "Fiber nonlinearity compensation by digital backpropagation of an entire 1.2 Tb/s superchannel using a full-field spectrally-sliced receiver," in *Tech. Digest of European Conference on Optical Communications*, 2013, paper Mo.3.D.5.
24. G. Liga, T. Xu, L. Galdino, R. Killay and P. Bayvel, "Digital back-propagation for high spectral efficiency Terabit/s superchannels," in *Tech. Digest of Optical Fiber Communications*, 2014, paper W2A.23.
25. T. Tanimura, T. Kato, R. Okabe, S. Oda, T. Richter, R. Elschner, C. Schmidt-Langhorst, C. Schubert, J. C. Rasmussen and S. Watanabe, "Coherent reception and 126 GHz bandwidth digital signal processing of CO-OFDM superchannel generated by fiber frequency conversion," in *Tech. Digest of Optical Fiber Communications*, 2014, paper Tu3A.1.
26. P. Poggiolini, G. Bosco, A. Carena, V. Curri, Y. Jiang, and F. Forghieri, "The GN-Model of fiber non-linear propagation and its applications," *J. Lightwave Technol.* **32**(4), 694–721 (2014).

## 1. Introduction

The quest for ever higher transmission rates in single mode optical fiber transmission has directed research efforts to (i) compensation of fiber nonlinearities or (ii) considering them as additional noise that can be mitigated using strong forward error correction (FEC) schemes together with judicious choice of the transmitted constellation (coded modulation) [1–3]. In the first approach digital backpropagation (DBP) [4–7] has proved to be effective in mitigating nonlinear distortion and increasing the effective received signal-to-noise ratio (SNR) at the decision gate. The principle of this technique is to digitally reverse the fiber channel transfer function using a zero-forcing approach, meaning that the distortion caused by nonlinear effects is forced to zero by the equalization process [8]. In multichannel DBP, the number of backpropagated channels is increased so that the backpropagated bandwidth approaches that of the transmitted signal field. This increases the effectiveness of the technique by providing more information about all the channels and their nonlinear interactions, including cross-phase modulation and four-wave mixing products generated by frequency components outside the bandwidth of the channel of interest.

A number of groups have already investigated in simulations the achievable improvements

with multichannel DBP when the entire signal field is backpropagated [9–14]. Significant improvements in both  $Q^2$  factor and reach have been achieved for PDM-16QAM modulation format compared to single channel DBP. However in these simulations the operation of the algorithm has always been assumed to be ideal. This means that backpropagation was performed with the same parameters as the simulated forward propagation in fiber including the same nonlinearity parameter  $\gamma$  as the one of the fiber (or the same nonlinear phase rotation per step), same number of steps per span and same sampling rate. While this is a correct approach for quantifying the theoretical benefits of this nonlinear compensation scheme, it has limitations due to the required discretisation in time and space of the reverse nonlinear operator. Also, ideal multichannel DBP operation requires significant computational efforts, indicating the necessity to search for a trade-off between complexity and performance.

Other works have investigated the impact of the sampling rate, number of steps per span or amount of nonlinear rotation per step on the DBP performance but only in the context of single channel DBP [4, 7, 15–17]. In [18–20] the effect of the number of steps per span has been studied for a low-complexity version of multichannel DBP taking into account only incoherent nonlinear effects (SPM and XPM) for coarsely spaced WDM channels. In this paper we present the first quantitative study of the efficacy of multichannel DBP jointly considering parameters such as step size, sampling rate, PMD and the bandwidth of the backpropagated signal, for spectrally efficient Nyquist-spaced WDM channels.

When multichannel DBP has been applied in experiments, the reported benefits have proved relatively low, typically less than 1 dB in  $Q^2$  factor for long-haul systems [21–23]. The factors which contribute to the discrepancy between the theoretically achievable DBP benefit and the gains experimentally realized have not yet been well identified or explained. In our previous work [24], it has been shown that limitations to the sampling rate and number of steps can reduce the effectiveness of multichannel DBP to below that of single channel DBP. In this paper, we focus on investigating the DSP and system parameters that can have an impact on multichannel DBP effectiveness and explore the discrepancy between the theoretically and experimentally achieved results. We first focus on the impact on the DBP algorithm performance with variation of operation parameters, such as nonlinear phase rotation per step, number of steps per span and sampling rate. Second, the impact of polarization mode dispersion (PMD) was studied as an additional limitation to the performance improvement enabled by multichannel DBP.

## 2. Transmission simulation configuration

To assess the effectiveness of multichannel DBP under different operating conditions we simulated a super-channel made up of 5 phase-locked 32 Gbaud channels with 33 GHz spacing, delivering a 1.2 Tbit/s raw transmission rate as in [24] and consistent with the experimental setup in [23]. However, in contrast to [24] where the aim was to explain previously reported experimental results [23], in this work we consider a system with an ideal transmitter and receiver yielding no back-to-back implementation penalty. The schematic of the simulated system is shown in Fig. 1. A  $2^{15} - 1$  long pseudo-random binary sequence (PRBS) was used to generate  $2^{16}$  Gray-encoded 16QAM symbols for each polarization. These symbols were Nyquist shaped using a root raised cosine pulse with 3% rolloff factor. The transmitted sequences were decorrelated with a delay of 256 symbols to emulate independent data transmission on each of the channels and the patterns on the two polarizations were decorrelated by half the sequence length. The different channels were modulated using a phase and frequency locked comb of lasers to ensure ideal synchronous detection for DBP. The transmission systems consists of 80.17 km spans of standard single-mode fiber with erbium doped fiber amplifier (EDFA) amplification (parameters shown in Table 1). The reference case

**Table 1. Parameters of the simulated system**

Parameter	Value
Attenuation coefficient ( $\alpha$ )	0.19 dB/km
Dispersion parameter ( $\beta_2$ )	17 ps/nm/km
Nonlinear coefficient ( $\gamma$ )	1.2 W <sup>-1</sup> km <sup>-1</sup>
PMD	0
Span length	80.17 km
Number of spans	40
EDFA Noise Figure	4.5 dB
Simulation bandwidth	512 GHz
SSF step size	500 m

considered throughout this work is a 40-span transmission (N=40 in Fig. 1), of total length 3206.8 km and representing the maximum achievable distance for a system with electronic dispersion compensation (EDC) only with a target bit error rate (BER) of  $10^{-2}$  (~7.34 dBQ). To ensure accuracy in the simulation of the fiber forward propagation, the overall signal field (165 GHz) was sampled at 16 samples per symbol, for an overall 512 GHz simulation bandwidth. The split-step Fourier (SSF) algorithm with a uniform 500 m step size was used to solve the nonlinear Schrödinger equation (NLSE).

The key DSP blocks used at the receiver are shown in Fig. 1. The coherent receiver was assumed to be ideal, with no bandwidth limitation, allowing for ideal detection of the in-phase and quadrature signal components on both polarizations. Two different possible approaches were considered for the analog-to-digital conversion before the application of the DSP, which we discuss in the following.

First, in Fig. 1(a), the backpropagation bandwidth was selected using a 1% root raised-cosine filter (digital filter block), allowing us to reject the unwanted out-of-band ASE noise. In this case the sampling rate is equal to the rate originally used to emulate the fiber propagation. We refer to the selected bandwidth for DBP as the “backpropagated” bandwidth, regardless of the sampling rate utilised to digitise it, which is required to be equal to or greater than the former in order not to incur linear aliasing effects. The difference between the selected signal bandwidth

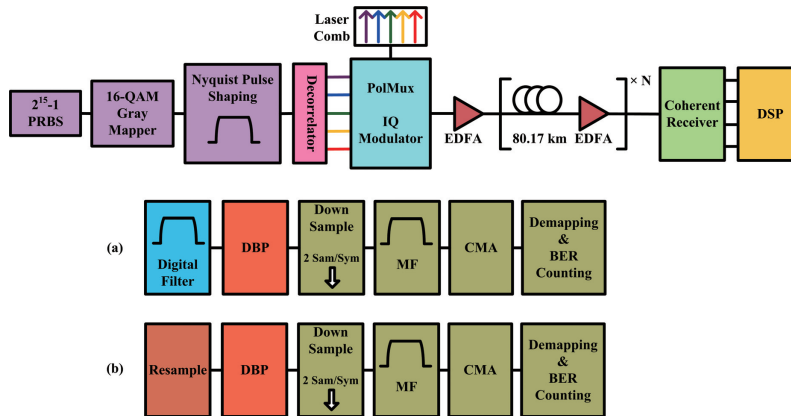


Fig. 1. Simulation schematic of 5x32 Gbaud Dual-Polarization (DP)-16QAM superchannel transmission with two different DSP schemes: (a) with full sampling rate DBP and (b) with limited sampling rate.

and the sampling rate used to digitise is crucial for the purpose of distinguishing between the benefits of including more frequency components into the DBP algorithm and the question of how accurately to digitise it before DBP is performed.

In the second approach (Fig. 1(b)) a resampler block was used to characterize the effects of limited sampling rate at which DBP can be operated. For both approaches DBP was followed by an additional resampling block converting the sampling rate to 2 samples/symbol, followed by a matched filter (MF) to select the central channel and polarization demultiplexing using a decision-directed, T/2-spaced, constant modulus algorithm (CMA) with 21 taps. Finally demapping of the symbols and bit error counting was carried out to assess the transmission performance of the central channel.

### 3. DSP optimization

#### 3.1. Impact of DSP parameters

The DBP algorithm digitally reverses the nonlinear transfer function induced by the signal propagation through the fiber. Ideal compensation of the induced distortion requires precise knowledge of the main optical fiber physical parameters involved, namely the chromatic dispersion parameter  $\beta_2$  and the nonlinearity parameter  $\gamma$ . In a real system this might not be trivial, so it is important to investigate the robustness of multichannel DBP when the parameters utilised in the signal processing deviate to some extent from the physical ones. In particular we focus on the variation of the  $\gamma$  parameter used in DBP ( $\gamma_{BP}$ ), assuming knowledge of the value of  $\beta_2$ , and reflecting the greater difficulty of accurately estimating the value of  $\gamma$  than that of the dispersion parameter.

The minimum number of steps per span required to accurately reverse the forward propagation is also key, due to the increase in the algorithm complexity associated with an arbitrarily small step size. The impact of varying the step size in DBP has been investigated previously in [4–7] only for single channel DBP. In [18–20] this has been investigated for a simplified implementation of DBP, where interchannel nonlinearity was compensated coupling the reverse NLSE for each channel. However, in a transmission scenario where the channels are nearly symbol rate spaced, this may lead to a significant penalty compared to a full-field DBP where the phase relationship between channels is preserved and the entire spectrum is jointly backpropagated.

Consistently with the experimental results shown in [23, 25], if a uniform step size SSF method is used to reverse fiber propagation, an increase of the DBP bandwidth requires a decrease in the step size to maintain the same accuracy, due to the larger variation induced in the propagated field by the chromatic dispersion effect.

Firstly in this work the performance of ideal multichannel DBP was investigated as a function of the backpropagated bandwidth. The performance metric used here throughout is the  $Q^2$  factor in dB calculated from the BER. In Fig. 2 the  $Q^2$  factor in dB is shown vs. launch power per channel for different values of the backpropagated bandwidth. In this case the DBP algorithm was operated at the same sampling rate used for the forward propagation (16 samples/symbol) and with the same number of steps per span (160, corresponding to a 500 m uniform step size).

It can be seen that the difference between the EDC only system and the fully backpropagated system (5 channels) in terms of maximum achievable  $Q^2$  factor is 3.8 dB and as high as 3 dB with respect to the single channel DBP. The 99 GHz (3 channels) DBP resulted in a 2.5 dB improvement with respect to the EDC-only system and approximately 1.5 dB gain with respect to the single channel DBP. It should be noted that, as expected, system performance improved with increased backpropagated bandwidth (in  $Q^2$ ), with slight saturation as we approach the full-field DBP bandwidth (0.83 dB per backpropagated channel between 0 and 3 channels and 0.65 dB per backpropagated channel between 3 and 5 channels). The reason for this saturation

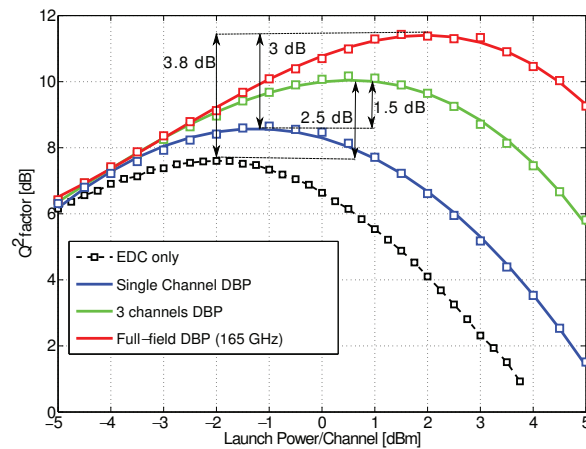


Fig. 2.  $Q^2$  factor vs. launch power per channel after 3206.8 km transmission with varying backpropagated bandwidth around the central channel. Continuous lines fit obtained results represented by markers.

is twofold: (i) the nonlinearity scaling logarithmically with the bandwidth [26] and (ii) the predominance in the effective SNR of the ASE-signal nonlinear interaction when the DBP bandwidth is close to the one of the entire field [10].

The results in Fig. 2 are achieved by ideally operating the algorithm for each backpropagated bandwidth at the expense of a high computational complexity and assuming knowledge of the  $\gamma$  parameter of the fiber. Since this is not always possible, the performance degradation due to suboptimal operation was studied next.

First the impact of the number of steps per span for different backpropagated bandwidths was

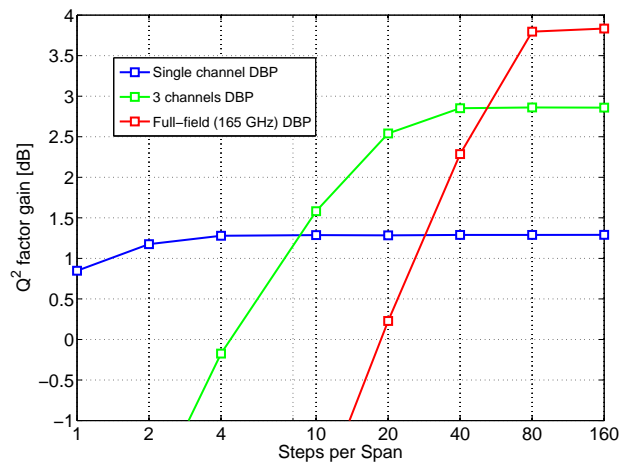


Fig. 3.  $Q^2$  factor gain versus number of steps per span after 3206.8 km transmission with varying backpropagated bandwidth around the central channel and  $\gamma_{BP}$  optimized for each value of the number of steps.

investigated, using the  $Q^2$  factor gain as a metric. The  $Q^2$  factor gain is defined as the difference in dB between  $Q^2$  factor achieved at optimum launch power for each backpropagated bandwidth and the optimum  $Q^2$  factor achieved with an EDC-only scheme.

In Fig. 3 we show the variation of the  $Q^2$  factor gain vs. the number of steps per span used for DBP. The value of  $\gamma_{BP}$  was optimised for each number of steps used, as the backpropagated bandwidth was varied between the single channel bandwidth (33 GHz) and the full transmitted bandwidth (165 GHz). It can be seen that increasing the bandwidth the DBP algorithm requires significantly greater number of steps per span or, equivalently, the step size needs to be decreased in order to achieve the expected performance improvement. Backpropagating a large bandwidth with an insufficiently short step size is not only ineffective but can be detrimental (i.e., negative  $Q^2$  gains in Fig. 3) as it introduces additional distortion to the signal due to the inaccurate inversion of the NLSE. In particular the three curves intersect at a given value of the number of steps which represents the minimum required value to correctly operate DBP for that given backpropagated bandwidth. Single channel DBP can be operated at 1 step per span with a penalty with respect to the optimal operation of just 0.5 dB, while at least 10 steps in

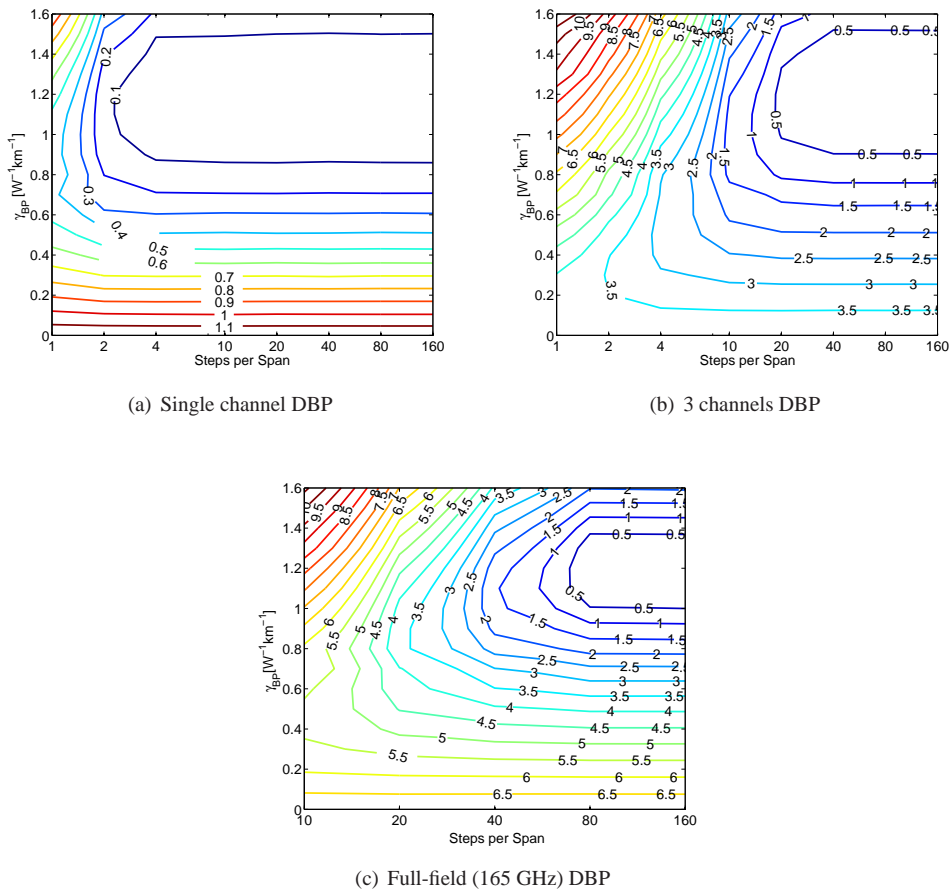


Fig. 4.  $Q^2$  factor optimization in number of steps per span and DBP nonlinear parameter  $\gamma_{BP}$  for (a) single channel case, (b) 3 channels and (c) full-field DBP. Labels indicate the  $Q^2$  factor penalty in dB compared to the maximum value achieved operating DBP at 160 steps/span and  $\gamma_{BP}=1.2 \text{ W}^{-1} \text{ km}^{-1}$ .



the case of 3 channel DBP and 80 steps for full-field DBP are needed to obtain significant gain. Specifically in the full-field case we observe that when operated with fewer than 20 steps per span the performance is worse than that achieved using an EDC only scheme.

The  $Q^2$  factor penalty, defined as the penalty from the optimal achievable  $Q^2$ , as a function of both  $\gamma_{BP}$  and the number of steps per span, was calculated from the simulations results and is shown in Fig. 4. It can be seen that, by fixing the number of steps per span below the ideal number to constrain computational complexity, the lowest penalty is achieved for values of  $\gamma_{BP}$  below that of the fiber, equivalent to an undercompensation of nonlinear phase shift per step. This is because, in the case of suboptimal step size, overcompensation leads to additional distortion accumulated over the entire link. As the step size is decreased, the optimum  $\gamma_{BP}$  converges to that of the fiber as expected.

### 3.2. Impact of sampling rate

Once the signal bandwidth to be backpropagated has been chosen, another important parameter to be investigated is the number of samples per second to be used for the detected signal digitisation. The complexity of the algorithm scales superlinearly with the number of samples per second  $N_s$  (complexity is dominated by the fast Fourier transform which scales as  $O(N_s \log_2(N_s))$ ), therefore a reduction of  $N_s$  is desirable. A lower bound on the sampling rate is given by the need to correctly reproduce the signal waveform without aliasing. While this is sufficient if we want to preserve the information of the analog signal in the digital domain when performing linear DSP, it may be insufficient if a nonlinear processing is performed. A higher sampling rate is necessary for the case of nonlinear propagation compared to the linear case, since the nonlinearity generates new frequency components which need to be captured without aliasing by the digital representation of the signal.

This concept is schematically illustrated in Fig. 5. The difference between a superchannel spectrum sampled at frequency  $F_s$  equal to the Nyquist rate (sampling rate equal to signal bandwidth) and the case where the spectrum has been oversampled by a factor of 2 is shown. The guard band between the replicas of the original spectrum (red spectra) allows the space for new DBP-generated out-of-band frequency components without incurring any aliasing.

It is now possible to quantify the sampling rate needed to correctly digitise the bandwidth to be backpropagated. For this purpose the number of steps per span was maintained to the ideal value of 160 as in the forward propagation (500 m step). The  $Q^2$  factor gain versus the sampling rate is plotted in Fig. 6. It is shown that for each backpropagated bandwidth there is a threshold sampling rate needed to obtain the optimal gain and it corresponds to approximately oversampling the backpropagated bandwidth by a factor of approximately 1.3. In our case,

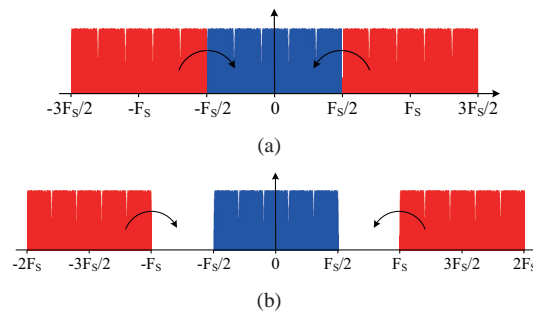


Fig. 5. Superchannel spectrum digitised at frequency  $F_s$  equal to (a) the Nyquist rate (sampling rate equal to signal bandwidth) and (b) twice the Nyquist rate.

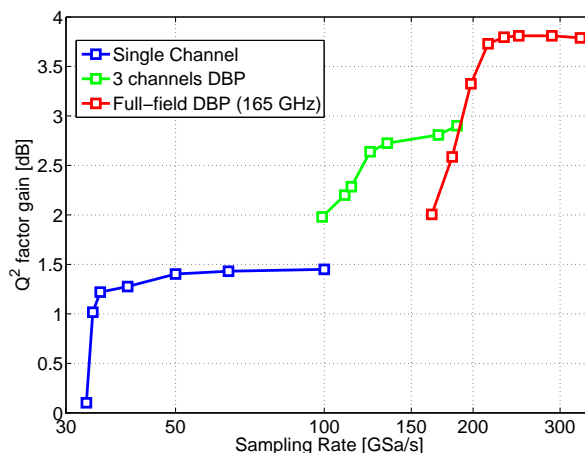


Fig. 6.  $Q^2$  factor gain with respect to EDC-only system versus sampling rate for different backpropagated bandwidths.

in order to observe the full advantage of the full-field backpropagation, we need to use a sampling rate greater than 200 GSa/s. Backpropagation of the entire spectrum of 5 channels sampled at the Nyquist rate (165 GSa/s) results in a performance worse than backpropagating just 3 channels at the same sampling rate. Therefore, as shown in [24], backpropagating an oversampled smaller bandwidth can result in better performance compared to a larger backpropagated bandwidth sampled at Nyquist rate. These results provide a criterion for the choice of the bandwidth (or the number of channels) to be backpropagated when the sampling rate is a system constraint.

#### 4. Impact of PMD

In addition to the effects of the choice of DSP parameters on the system performance as discussed above, another system parameter which has a significant effect on the performance of DBP is PMD. Although not explicitly investigated in experiments which have applied multichannel DBP, the stochastic nature of the PMD process is known to affect DBP performance [11, 12].

The significance of this is shown by resimulating the system in Fig. 6 with a varying amount of PMD (PMD parameter varying from 0 to 1 ps/ $\sqrt{\text{km}}$ ). Multichannel backpropagation was performed in this case with optimal operation parameters. Because of the randomness of the PMD process, 10 different realisations of the polarisation evolution through the fiber were simulated for each PMD parameter and the resultant average BER is used to calculate the  $Q^2$  factor. The  $Q^2$  factor gain versus a varying amount of PMD was then calculated and is shown in Fig. 7. Error bars are also used to indicate the standard deviation of the obtained random values. We fixed the reference for the presented gains to the EDC-only system with its respective PMD value. However, for the different cases without or with any of the studied values of PMD we did not notice a significant variation in the  $Q^2$  factor calculated at optimum launch power (within 0.3 dB). This difference is more significant in a regime of stronger nonlinearity. The results in Fig. 7 show that PMD has a more detrimental effect as the backpropagated bandwidth is increased. For a relatively small value of the PMD parameter (0.01 ps/ $\sqrt{\text{km}}$ ) backpropagating the full-field results in a penalty of 0.5 dB as compared to the achievable gains shown in Fig. 1 and Fig. 2. For a typical value of the PMD parameter (0.1 ps/ $\sqrt{\text{km}}$ ) the  $Q^2$  factor gain decreases

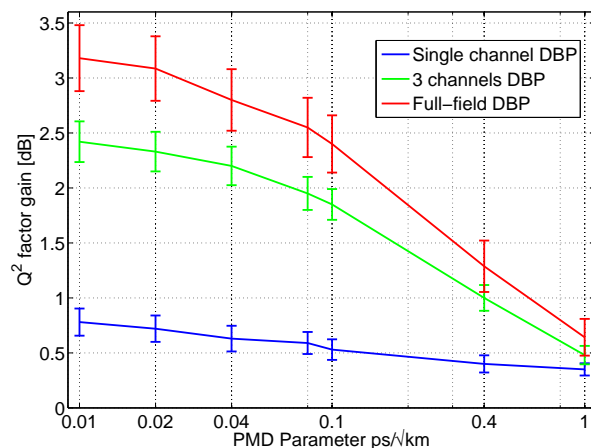


Fig. 7.  $Q^2$  factor gain with respect to EDC-only system versus PMD parameter, for varying backpropagated bandwidth. Error bars signify the standard deviation of the obtained values.

to 2.5 dB, 1.3 dB less than the optimal gain value and the gap with respect to the gain achieved by 3 channels DBP reduces to 0.5 dB. As the PMD parameter is increased the gain we expect by increasing the backpropagated bandwidth decreases until it becomes negligible for a PMD parameter equal to  $1 \text{ ps}/\sqrt{\text{km}}$ . This effect can be explained due to the inability of DBP to keep track at each step of the random polarisation rotations of each frequency components in the backpropagated spectrum. As a result, inter-channel nonlinear interactions strongly depending on the polarisation state of each of the channels cannot be properly undone [11, 12].

## 5. Conclusions

The impact of the key operation parameters of multichannel DBP applied to high spectral efficiency transmission systems was investigated.

In terms of the number of steps per span used to backpropagate the signal it was found that this must be increased as the backpropagated bandwidth increases and the benefit of backpropagating large bandwidths can be reduced to that of single channel DBP, or worse, if a suboptimal step size is used, due to the inaccurate compensation of the nonlinearity. Specifically, in our 165 GHz (5 channels) full-field backpropagation, it was shown that more than 80 steps/span (approx. step size of 1 km) were required to achieve optimal performance of 3.8 dB higher  $Q^2$  factor than EDC-only and 3 dB with respect of single channel DBP. When multichannel DBP is performed optimally but fiber PMD effects are taken into account we found that, for typical values of the PMD parameter, the beneficial effects of multichannel DBP reduce significantly as the backpropagated bandwidth is increased. Therefore, in the presence of PMD, backpropagating larger portions of bandwidth beyond a certain value becomes ineffective to improve the transmission performance of the system.

## Acknowledgments

The authors would like to thank Dr. Domaniç Lavery for helpful discussions. Financial support from the UK EPSRC Programme Grant UNLOC (Unlocking the capacity of optical communications) EP/J017582/1 and Huawei Technologies is gratefully acknowledged.